Yinggan Tang
Institute of Electrical Engineering;
National Engineering Research Center for
Equipment and Technology of Cold Strip Rolling,
Yanshan University,
Qinhuangdao, Hebei 066004, China
e-mail: ygtang@ysu.edu.cn

Ying Wang
Institute of Electrical Engineering,
Yanshan University,
Qinhuangdao, Hebei 066004, China

Mingyu Han
Institute of Electrical Engineering,
Yanshan University,
Qinhuangdao, Hebei 066004, China

Qiusheng Lian
School of Information Science and Engineering,
Yanshan University,
Qinhuangdao, Hebei 066004, China

Adaptive Fuzzy Fractional-Order Sliding Mode Controller Design for Antilock Braking Systems

Antilock braking system (ABS) has been designed to attain maximum negative acceleration and prevent the wheels from locking. Many efforts had been paid to design controller for ABS to improve the brake performance, especially when road condition changes. In this paper, an adaptive fuzzy fractional-order sliding mode controller (AFFOSMC) design method is proposed for ABS. The proposed AFFOSMC combines the fractional-order sliding mode controller (FOSMC) and fuzzy logic controller (FLC). In FOSMC, the sliding surface is PD^{α}, which is based on fractional calculus (FC) and is more robust than conventional sliding mode controllers. The FLC is designed to compensate the effects of parameters varying of ABS. The tuning law of the controller is derived based on Lyapunov theory, and the stability of the system can be guaranteed. Simulation results demonstrate the effectiveness of AFFOSMC for ABS under different road conditions.
[DOI: 10.1115/1.4032555]

Keywords: antilock braking system, fractional-order, sliding mode control, fuzzy control, adaptive

1 Introduction

Nowadays, cars have become a kind of necessary transportation. To achieve high safety, efficiency, and comfort, many sophisticated techniques had been developed and introduced into cars. These techniques include ABS, traction control, electronic stability program, and so on [1]. Among these, ABS is one of the most popular and common systems that improve the safety of cars [2]. The primary goal of ABS is to improve the braking effectiveness by regulating the wheel slip λ at the optimal point and prevent wheels from lockuping. The wheel lockup occurs when a vehicle is braked on a slippery road or during emergency braking. It is a dangerous thing if the wheel is locked up because the car will lose the directional stability and lead to lateral sliding.

To avoid lockup, many ABS controller design methods have been proposed. A model-based approach was used to search for the optimum brake torque via sliding modes in Ref. [3]. A feedback linearization was adopted to design a slip controller in Ref. [4]. A discrete-time controller for ABS was given in Ref. [5]. Jing et al. presented a switched control strategy for an ABS, which has conventional hydraulic actuators equipped with on/off valves [6]. In Ref. [7], an eddy current approach was used to design an optimal robust controller for a contactless brake system, and so on.

Although many works had been done, ABS controller design is still a difficult task. Existing methods in the literature share two shortcomings. The first is that most of the ABS controllers are designed based on integer calculus (IC), i.e., the differentiation and integration are performed in integer order. The second is that they all require an accurate model of ABS system. In fact, the accurate model is difficult to obtain because high nonlinearities and uncertainties, which are caused by unknown environmental parameters, exist in the mathematical model of ABS. For the first problem, since IC is local and cannot describe a system with historical memory, the FC was introduced into control system to enhance the performance of control system [8]. The FC is regarded as an extension of regular IC to noninteger case [9,10]. Compared to IC, FC is nonlocal, which makes it suitable to describe system with long-memory. Several fractional controllers, such as tilted proportional and integral controller [11], CRONE controller [12], fractional-order proportional integral derivative controller [13], had been proposed. On the other hand, the FC was also integrated into sliding mode control (SMC) to obtain better performance. In Ref. [14], Efe developed an SMC scheme using fractional-order reaching law for quadrotor-type unmanned aerial vehicle. To improve the robustness of fuzzy SMC, a novel parameter adjustment scheme utilizing fractional integration was proposed in Ref. [15]. In Ref. [16], an SMC with fractional sliding surface was proposed. For the second problem, the designed controller should have the ability of dealing with uncertainties and nonlinearities. Fuzzy logical control (FLC) is a better solution to this problem. FLC uses linguistic information, which can model the qualitative aspects of human knowledge with several advantages such as robustness, universal approximation theorem, and rule-based algorithm [17–20]. FLC can tackle the unknown part of system model, therefore, FLC is applied to ABS to solve the problem of model uncertainty. In Ref. [21], Layne et al. designed a fuzzy learning controller for ABS. Mauer designed an FLC for ABS in Ref. [22]. However, these approaches need a large amount of fuzzy rules, and they increase the complexity of design procedure. In consideration of high robustness of SMC, many researchers combined FC and SMC and proposed fuzzy control design methods based on SMC, called fuzzy sliding mode control (FSMC). In Ref. [23], Kim and Lee designed a fuzzy controller with fuzzy sliding surface and applied it to a nonlinear time-varying system. In Ref. [24], an SMC theory-based learning algorithm was applied to type-2 fuzzy neural networks. In Ref. [1], a robust FSMC was proposed and applied to ABS controller design.

In this paper, an AFFOSMC method is proposed for ABS. The present work is based on our previous work in Ref. [25]. In Ref. [25], we design the FOSMC for ABS by integrating FC into SMC. Although the performance of FOSMC is superior to conventional SMC, FOSMC still cannot effectively deal with model uncertainties and disturbances. Therefore, we adopt the idea of FLC to enhance the performance of FOSMC. In our proposed control method, an FOSMC with PD^{α} sliding surface is designed based on the nominal model of ABS, and the FLC is designed to compensate the effect of parameter variation of ABS. The proposed method improves the robustness just like fractional-order

Contributed by the Dynamic Systems Division of ASME for publication in the Journal of Dynamic Systems, Measurement, and Control. Manuscript received July 21, 2015; final manuscript received January 12, 2016; published online February 17, 2016. Assoc. Editor: Heikki Handroos.

sliding-mode control, and reduces the chattering phenomenon immensely just like FSMC, besides the proposed method regulates the fuzzy rules automatically just like adaptive fuzzy control.

The rest of this paper is organized as follows: The basic of FC is briefly reviewed in Sec. 2. In Sec. 3, the mathematical model of ABS is introduced. The design procedure of sliding mode controller based on fractional-order PD^{α} sliding surface is described in Sec. 4. The design procedure of AFFOSMC is described in detail in Sec. 5. Simulation results are given in Sec. 6. Finally, the concluding remarks are presented in Sec. 7.

2 The Basics of FC

2.1 Definitions of Fractional Derivative and Integral. FC is a generalization of the integration and differentiation to a noninteger order integrodifferential operator ${}_a\mathrm{D}_t^{\alpha}$, where a and t are the lower and upper limits and $\alpha(\alpha \in R)$ is the order of the operation [26]. The continuous fractional integrodifferential operator is defined as

$$ {}_a\mathrm{D}_t^{\alpha} = \begin{cases} \dfrac{\mathrm{d}^{\alpha}}{\mathrm{d}t^{\alpha}}, & \Re(\alpha) > 0 \\ 1, & \Re(\alpha) = 0 \\ \displaystyle\int_a^t (\mathrm{d}\tau)^{-\alpha}, & \Re(\alpha) < 0 \end{cases} \tag{1} $$

where α is a complex number and $\Re(\alpha)$ is the real part of α. There are several definitions for fractional derivative. Grünwald-Letnikor (GL), Riemann-Liouville (RL), and Caputo definitions are commonly used. The GL definition [26] is

$$ {}_a\mathrm{D}_t^{\alpha} f(t) = \lim_{h\to 0} h^{-\alpha} \sum_{j=0}^{[(t-a)/h]} (-1)^j \binom{\alpha}{j} f(t - jh) \tag{2} $$

where h is the time increment, $[\cdot]$ means the integer part, and

$$ \binom{\alpha}{j} = \frac{\Gamma(\alpha+1)}{\Gamma(j+1)\Gamma(\alpha-j+1)} \tag{3} $$

with Gamma function $\Gamma(\cdot)$. The RL definition [26] is

$$ {}_a\mathrm{D}_t^{\alpha} f(t) = \frac{1}{\Gamma(n-\alpha)} \frac{\mathrm{d}^n}{\mathrm{d}t^n} \int_a^t \frac{f(\tau)}{(t-\tau)^{\alpha-n+1}} \mathrm{d}\tau \tag{4} $$

where n is the first integer which is not less than α, i.e., $n-1 \le \alpha < n$. The Caputo definition [26] is given by

$$ {}_a\mathrm{D}_t^{\alpha} f(t) = \frac{1}{\Gamma(n-\alpha)} \int_a^t \frac{f^{(n)}(\tau)}{(t-\tau)^{\alpha-n+1}} \mathrm{d}\tau \tag{5} $$

In the analysis and design of control systems, Laplace transform is a very popular tool. The Laplace transform of the RL fractional derivative, Eq. (4), is

$$ \int_0^{\infty} {}_0\mathrm{D}_t^{\alpha} f(t) e^{-st} \mathrm{d}t = s^{\alpha} \mathcal{L}\{f(t)\} - \sum_{k=0}^{n-1} s^k \, {}_0\mathrm{D}_t^{\alpha-k-1} f(t)|_{t=0} \tag{6} $$

and the Laplace transform of the Caputo fractional derivative, Eq. (5), is given by

$$ \int_0^{\infty} {}_0\mathrm{D}_t^{\alpha} f(t) e^{-st} \mathrm{d}t = s^{\alpha} \mathcal{L}\{f(t)\} - \sum_{k=0}^{n-1} s^{\alpha-k-1} f^{(k)}(0) \tag{7} $$

where $\mathcal{L}\{\cdot\}$ denotes the Laplace operator. Therefore, under zero initial conditions, the fractional integral operator with order α can be represented by the transfer function $F(s) = 1/s^{\alpha}$ in the frequency domain.

2.2 Approximation of Fractional Derivative. In practice, it is necessary to calculate the numerical solution of fractional systems described by fractional differential equations. However, it is difficult to obtain the exact solution of fractional differential equations in most cases. Approximation methods were widely adopted in practice. One popular approximation is done in frequency domain, in which the transfer functions involving fractional powers of s are approximated with the usual (integer order) transfer functions with a similar behavior. Other approximations were done through numerical solution of fractional differential equations. In Ref. [27], a numerical method for fractional differential equations was proposed based on Adams–Bashforth–Moulton [28] type predictor–corrector scheme. In this paper, a frequency approximation method by Oustaloup [8] is adopted. The Oustaloup approximation makes use of a recursive distribution of poles and zeroes. The approximating transfer function is given by

$$ s^{\alpha} \approx K \prod_{n=-N}^{N} \frac{1 + (s/\omega_{z,n})}{1 + (s/\omega_{p,n})}, \quad \alpha > 0 \tag{8} $$

where $2N+1$ is the number of poles and zeros chosen beforehand, K is the gain that such that both sides of Eq. (8) shall have unit gain at 1 rad/s. $\omega_{z,n}$ and $\omega_{p,n}$ are given as

$$ \omega_{z,n} = \omega_b \left(\frac{\omega_h}{\omega_b}\right)^{\frac{n+N+(1-\alpha)/2}{2N+1}} \tag{9} $$

$$ \omega_{p,n} = \omega_b \left(\frac{\omega_h}{\omega_b}\right)^{\frac{n+N+(1+\alpha)/2}{2N+1}} \tag{10} $$

In Eqs. (9) and (10), ω_b and ω_h are the lower and upper limits of frequency of approximation, usually $\omega_b\omega_h = 1$, and thus, $K = \omega_h^{\alpha}$.

The case $\alpha < 0$ can be handled by inverting Eq. (8). For $|\alpha| > 1$, the approximation becomes unsatisfactory; for that reason, it is usual to split fractional powers of s like this

$$ s^{\alpha} = s^n s^{\delta}, \quad \alpha = n + \delta, n \in \mathbb{Z}, \delta \in [0, 1] \tag{11} $$

As a result, only the latter term has to be approximated.

2.3 Stability of Fractional-Order Systems. The stability of fractional-order systems is of main interest in control theory. This issue has been addressed by several authors. In Ref. [29], Matignon stated that the following autonomous system

$$ {}_0\mathrm{D}_t^{\alpha} x = Ax, x(0) = x_0 \tag{12} $$

where α is differential order, $x \in R^n$ and $A \in R^{n\times n}$, are asymptotically stable if $|\arg(\mathrm{eig}(A))| > \alpha\pi/2$. In this case, each component of the states decays toward 0 like $t^{-\alpha}$. Also, this system is stable if $|\arg(\mathrm{eig}(A))| \ge \alpha\pi/2$ and those critical eigenvalues that satisfy $|\arg(\mathrm{eig}(A))| = \alpha\pi/2$ have geometric multiplicity one. Figure 1 shows the stable region for $0 < \alpha < 2$. Obviously, the stable region

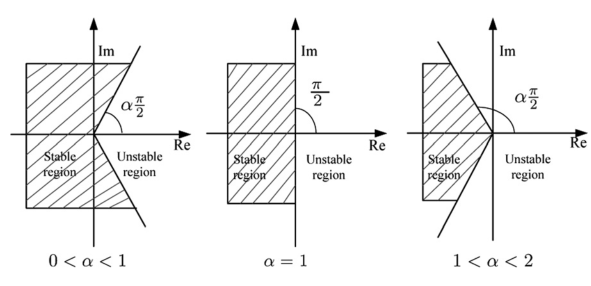

Fig. 1 Stability region of fractional system

of fractional system with $0<\alpha<1$ is the largest than that of the other two cases.

3 Mathematical Model of ABS

The dynamic equations of ABS are the result of Newton's law applied to the wheels and the vehicle [21]. The vehicle dynamic during braking is obtained as follows:

$$\dot{V}_v(t) = \frac{-1}{M}\left[4F_t(t) + B_v V_v + F_\theta(\theta)\right] \tag{13}$$

$$\dot{\omega}_\omega = \frac{1}{J_\omega}\left[-T_b(t) - B_\omega \omega_\omega(t) + T_t(t)\right] \tag{14}$$

The description of different forces in Eqs. (13) and (14) is given as follows:

$$F_\theta(\theta) = \mathrm{Mg}\sin(\theta) \tag{15}$$

$$F_t(t) = \mu(\lambda, V_v) N_v(\theta) \tag{16}$$

$$N_v(\theta) = \frac{\mathrm{Mg}}{4}\cos(\theta) \tag{17}$$

$$T_t(t) = F_t(t) R_\omega \tag{18}$$

where θ is the angle of inclination of the road, g is the gravitational acceleration constant, $N_v(\theta)$ is the nominal wheel reaction force applied to the wheel, $\mu(\lambda, V_v)$ is the coefficient of friction, R_ω represents the radius of the wheel.

Let $\omega_v(t)$ be the angular velocity of the vehicle, it is calculated as

$$\omega_v(t) = \frac{V_v(t)}{R_\omega} \tag{19}$$

The wheel slip is defined as [30]

$$\lambda(t) = \frac{\omega_v(t) - \omega_\omega(t)}{\omega_v(t)} \tag{20}$$

Taking the time derivative of Eq. (20), one can obtain

$$\dot{\lambda} = \frac{(1-\lambda)\dot{\omega}_v - \dot{\omega}_\omega}{\omega_v} \tag{21}$$

Substituting Eqs. (13), (14), and (19) into Eq. (21) one has,

$$\dot{\lambda} = F_p(\lambda) + G_p u(t) \tag{22}$$

where

$$F_p(\lambda) = \left(\frac{4F_t + B_v R_\omega \omega_v + F_\theta}{M_v R_\omega \omega_v}\right)\lambda - \frac{(4F_t + B_v R_\omega \omega_v + F_\theta)/M_v R_\omega + (T_t - B_\omega W_\omega)/J_\omega}{\omega_v} \tag{23}$$

represents the nonlinear dynamic function, and

$$G_p = 1/J_\omega \tag{24}$$

denotes the control gain, and

$$u(t) = T_b(t)/\omega_v \tag{25}$$

is the control effort. If all the parameters of system (22) are well known, we can obtain the nominal model of the system as

$$\dot{\lambda} = F_n(\lambda) + G_n u(t) \tag{26}$$

where $F_n(\lambda)$, G_n represent the nominal values of $F_p(\lambda)$, G_p, respectively. The nominal values of the system parameters are measured at $\mu(\lambda, V_v)=0.75$ and $\theta=0$ [31]. When the uncertainties occur, the system (22) is rewritten as follows:

$$\begin{aligned}\dot{\lambda} &= [F_n(\lambda) + \triangle F(\lambda)] + [G_n + \triangle G]u(t)\\ &= F_n(\lambda) + G_n u(t) + d,\end{aligned} \tag{27}$$

where $\triangle F(\lambda)$, $\triangle G$ denote the uncertainties, d represents the lump uncertainty and $|d| \le \rho,\ \rho > 0$.

4 SMC Based on Fractional-Order PD$^\alpha$ Sliding Surface

In the following, an FOSMC controller is designed for ABS. To do this, we make the following assumption.

Assumption 1. *The velocities of the vehicle and wheel can be measured.*

The ABS structure with FOSMC system is shown in Fig. 2. The control purpose is to make the slip track the desired value under the designed control law. Let the tracking error be

$$\lambda_e(t) = \lambda_d(t) - \lambda(t) \tag{28}$$

where $\lambda_d(t)$ represents the desired trajectory, $\lambda(t)$ denotes the actual output. Define a fractional-order PD$^\alpha$ sliding surface as

$$s(t) = \lambda_e(t) + k\mathrm{D}^\alpha \lambda_e(t), k > 0 \tag{29}$$

Let $s=0$, one can obtain that

$$\frac{1}{k}\lambda_e(t) = -\mathrm{D}^\alpha \lambda_e(t) \tag{30}$$

According to Eq. (12), we have $A = -1/k$, and $|\arg(\mathrm{eig}(A))| = \pi$. When $0 < \alpha < 2$, $|\arg(\mathrm{eig}(A))| > \alpha\pi/2$ is constant established. Therefore, the dynamics of $s(t)=0$ are asymptotically stable.

The FOSMC is designed as

$$u_{\mathrm{FOSMC}}(t) = u_{\mathrm{eq}}(t) + u_{\mathrm{rb}}(t) \tag{31}$$

where $u_{\mathrm{eq}}(t)$ denotes the equivalent controller, which is represented as

$$u_{\mathrm{eq}}(t) = G_n{}^{-1}[\dot{\lambda}_d(t) + k\mathrm{D}^{\alpha+1}\lambda_e(t) - F_n(\lambda)] \tag{32}$$

and $u_{\mathrm{rb}}(t)$ is the hitting controller. It is designed as

$$u_{\mathrm{rb}}(t) = G_n{}^{-1}[\rho\,\mathrm{sgn}(s(t))] \tag{33}$$

where $\mathrm{sgn}(\cdot)$ is a sign function. The hitting controller is used to dispel the system uncertainties. Substituting Eqs. (31)–(33) into Eq. (27), one can obtain

$$\dot{\lambda}_e(t) + kD^{\alpha+1}\lambda_e(t) = -\rho\,\mathrm{sgn}(s(t)) - d = \dot{s}(t) \tag{34}$$

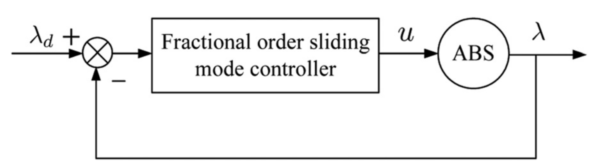

Fig. 2 ABS structure with FOSMC controller

Choosing the following Lyapunov function:

$$V_1(t) = \frac{1}{2}s^2(t) \tag{35}$$

Differentiating Eq. (35) and using Eq. (34), one has

$$\begin{aligned}\dot{V}_1 &= s(t)\dot{s}(t) \\ &= s(t)(-\rho \operatorname{sgn}(s(t)) - d) \\ &= -ds(t) - \rho|s(t)| \le |d||s(t)| - \rho|s(t)| \\ &= |s(t)|(|d| - \rho) \le 0.\end{aligned} \tag{36}$$

It is clear that the designed FOSMC can guarantee the stability of the whole system in Lyapunov sense.

5 Adaptive Fuzzy Fractional-Order SMC Design

To obtain high control performance, it is necessary to know the accurate mathematical model of ABS. However, the accurate model is difficult to know because of the uncertainties. Therefore, an AFFOSMC design method is proposed for ABS in this paper. The ABS system with AFFOSMC is shown in Fig. 3.

5.1 FSMC. Assume that there are n rules in a fuzzy rule base, and every rule has the following form:

Rule i. *If s_1 is A_1^i and s_2 is A_2^i then u is p_i.*
where s_1 and s_2 are the input variables of the fuzzy system. In this paper, we select $s_1 = s$ and $s_2 = \dot{s}$ (s is the sliding mode surface), u is the output variable of the fuzzy system, A_1^i and A_2^i are Gaussian-type membership functions, P_i are the singleton control actions for $i = 1,2,\ldots, n$. In this paper, center-of-gravity is adopted as the defuzzification method. Thus, the output, i.e., the fuzzy controller can be obtained as

$$u = W^T(s_1, s_2)P \tag{37}$$

where $P = [p_1, p_2, \ldots, p_n]^{\mathrm{T}}$ is the parameter vector and $W(s_1, s_2) = [w_1(s_1, s_2), w_2(s_1, s_2), \ldots, w_n(s_1, s_2)]^{\mathrm{T}}$ is the regressive vector, there into

$$w_i(s_1, s_2) = \frac{\mu_{A_1^i(s_1)}\mu_{A_2^i(s_2)}}{\sum \mu_{A_1^i(s_1)}\mu_{A_2^i(s_2)}} \tag{38}$$

5.2 AFFOSMC Controller. If the parameters of the system (22) are well known, an ideal controller can be designed as

$$u_{\text{ideal}}(t) = G_p^{-1}[\dot{\lambda}_d(t) + k\mathrm{D}^{\alpha+1}\lambda_e(t) - F_p(\lambda)] \tag{39}$$

Substituting Eq. (39) into Eq. (22), the result is obtained as follows:

$$\dot{\lambda}_e(t) + k\mathrm{D}^{\alpha+1}\lambda_e(t) = 0 \tag{40}$$

As long as we choose appropriate k to meet the coefficients of a Hurwitz polynomial, it makes clear that $\lim_{t\to\infty} \lambda_e(t) = 0$. That is to say, the ideal controller can fulfill the control task. However, the ideal controller cannot be precisely obtained because the parameters of the system may be unknown or perturbed. To overcome this drawback, a fuzzy controller is designed to approximate the error between the ideal controller $u_{\text{ideal}}(t)$ and the equivalent controller $u_{\text{eq}}(t)$. There is an optimal fuzzy controller $u_{fz}^*(s, \dot{s}, P^*)$ in the form of Eq. (37) to satisfy

$$u_{\text{ideal}}(t) - u_{\text{eq}}(t) = u_{\text{fz}}^*(s, \dot{s}, P^*) + \varepsilon = W^T P^* + \varepsilon \tag{41}$$

where ε is the approximation error satisfying $|\varepsilon| \le E$. Let $\hat{u}_{fz}(s, \dot{s}, \hat{P})$ be the estimation of $u_{\text{fz}}^*(s, \dot{s}, P^*)$, i.e.,

$$\hat{u}_{fz}(s, \dot{s}, \hat{P}) = W^T\hat{P} \tag{42}$$

where $\hat{P}$ is the estimation of P^*. The AFFOSMC is designed as

$$u(t) = u_{\text{eq}}(t) + \hat{u}_{\text{fz}}(s, \dot{s}, \hat{P}) + u_{\text{rb}}(s) \tag{43}$$

where the fuzzy controller $\hat{u}_{\text{fz}}(s, \dot{s}, \hat{P})$ is designed to approximate the error between u_{ideal} and $u_{\text{eq}}(t)$, $u_{\text{rb}}(s)$ is the robust controller to compensate the error between $\hat{u}_{\text{fz}}(s, \dot{s}, \hat{P})$ and $u_{\text{ideal}}(t) - u_{\text{eq}}(t)$. Substituting Eq. (43) into Eq. (22), it is obtained that

$$\dot{\lambda}(t) = F_p(\lambda) + G_p[u_{\text{eq}}(t) + \hat{u}_{fz}(s, \dot{s}, \hat{P}) + u_{\text{rb}}(s)] \tag{44}$$

Multiplying Eq. (39) with G_p, and added to Eq. (44), it can be obtained that

$$\begin{aligned}\dot{\lambda}_e(t) + k\mathrm{D}^{\alpha+1}\lambda_e(t) &= G_p[u_{\text{ideal}} - u_{\text{eq}} - \hat{u}_{\text{fz}} - u_{\text{rb}}] \\ &= \dot{s}\end{aligned} \tag{45}$$

Let $\tilde{u}_{\text{fz}} = u_{\text{ideal}} - u_{\text{eq}} - \hat{u}_{\text{fz}}$, $\tilde{P} = P^* - \hat{P}$. Subtracting Eq. (42) from Eq. (41), it has

$$\tilde{u}_{fz} = W^T\tilde{P} + \varepsilon \tag{46}$$

Then, we have the following results.

Theorem 1. *The AFFOSMC controller presented in Eq. (43) with adaptive laws, Eqs. (47) and (48), and robust controller (49) can guarantee the stability of the system*

$$\dot{\hat{P}} = -\dot{\tilde{P}} = \eta_1 s(t)W \tag{47}$$

$$\dot{\hat{E}} = -\dot{\tilde{E}} = \eta_2|s(t)| \tag{48}$$

$$u_{\text{rb}} = \hat{E}\operatorname{sgn}(s(t)) \tag{49}$$

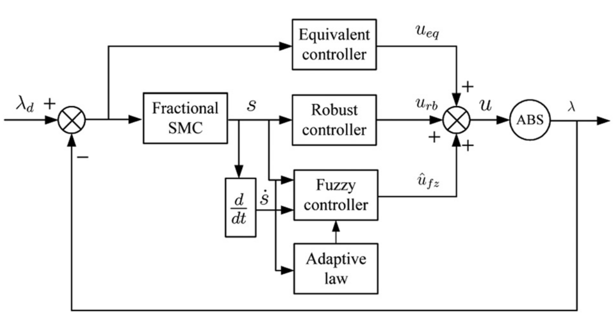

Fig. 3 ABS with AFFOSMC controller

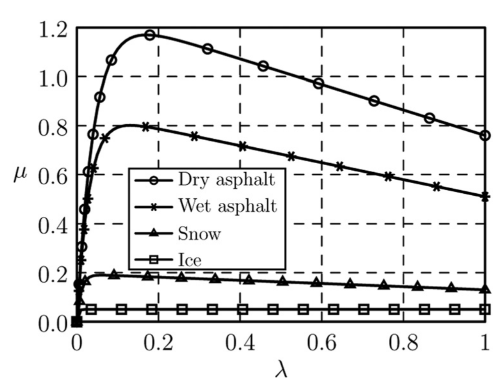

Fig. 4 Coefficient of road friction versus wheel slip ratio

where $\tilde{E} = E - \hat{E}$, $\hat{E}$ is the estimation of the bound E, η_1 and η_2 are positive constants.

Proof. Define Lyapunov function as

$$V_2 = \frac{1}{2}s^2 + \frac{G_p}{2\eta_1}\tilde{P}^T\tilde{P} + \frac{G_p}{2\eta_2}\tilde{E}^2 \tag{50}$$

Differentiating Eq. (50) with respect to time, it is obtained that

$$\begin{aligned}\dot{V}_2 &= s(t)\dot{s}(t) + \frac{G_p}{\eta_1}\dot{\tilde{P}}^T\tilde{P} + \frac{G_p}{\eta_2}\tilde{E}\dot{\tilde{E}}\\ &= s(t)G_p\left[W^T\tilde{P} + \varepsilon - u_{\mathrm{rb}}(s)\right] + \frac{G_p}{\eta_1}\dot{\tilde{P}}^T\tilde{P} + \frac{G_p}{\eta_2}\tilde{E}\dot{\tilde{E}}\\ &= G_p\left(sW^T + \frac{\dot{\tilde{P}}^T}{\eta_1}\right)\tilde{P} + sG_p(\varepsilon - u_{\mathrm{rb}}(s)) + \frac{G_p}{\eta_2}\tilde{E}\dot{\tilde{E}}\\ &= sG_p\varepsilon - G_pE|s(t)|\\ &\le G_p|s(t)|(|\varepsilon| - E) \le 0\end{aligned} \tag{51}$$

□

6 Numerical Results

To demonstrate the effectiveness of the proposed AFFOSMC controller, simulation studies are performed. For the purpose of comparison, three different controllers including SMC with PI sliding mode surface, SMC with fractional PD$^\alpha$ sliding mode surface, and the proposed AFFOSMC controller are implemented.

In simulation, the parameters of ABS are selected as in Ref. [32], i.e., $M = 4 \times 342$ kg, $B_v = 6$ Ns, $J_\omega = 1.13$ Nms^2, $R_\omega = 0.33$ m, $B_\omega = 4$ Ns, $g = 9.8$ m/s^2. Figure 4 shows the relationship between road coefficient μ and slip λ in different road conditions. From Fig. 4, it can be seen that the choice of the reference slip at 0.2 is relatively appropriate because the friction coefficient for different road conditions is maximized near $\lambda = 0.2$. And the maximum braking torque is limited to 1500 Nm. In addition, simulation is stopped at the point where the vehicle velocity drops to 5 m/s, the reason is that the wheel and vehicle's velocities are nearly zero at low-speed, and the magnitude of slip tends to infinity as the vehicle speed approaches zero. When the vehicle speed reaches 20 m/s, the braking action is applied. In addition, to reduce the chattering phenomenon, a saturation function is used to replace the signum function usually. The saturation function is described as

$$\mathrm{sat}\left(\frac{s}{\phi}\right) = \begin{cases}\mathrm{sgn}\left(\frac{s}{\phi}\right), & \left|\frac{s}{\phi}\right| \ge 1\\ \frac{s}{\phi}, & \left|\frac{s}{\phi}\right| < 1\end{cases} \tag{52}$$

where ϕ is width of boundary layer.

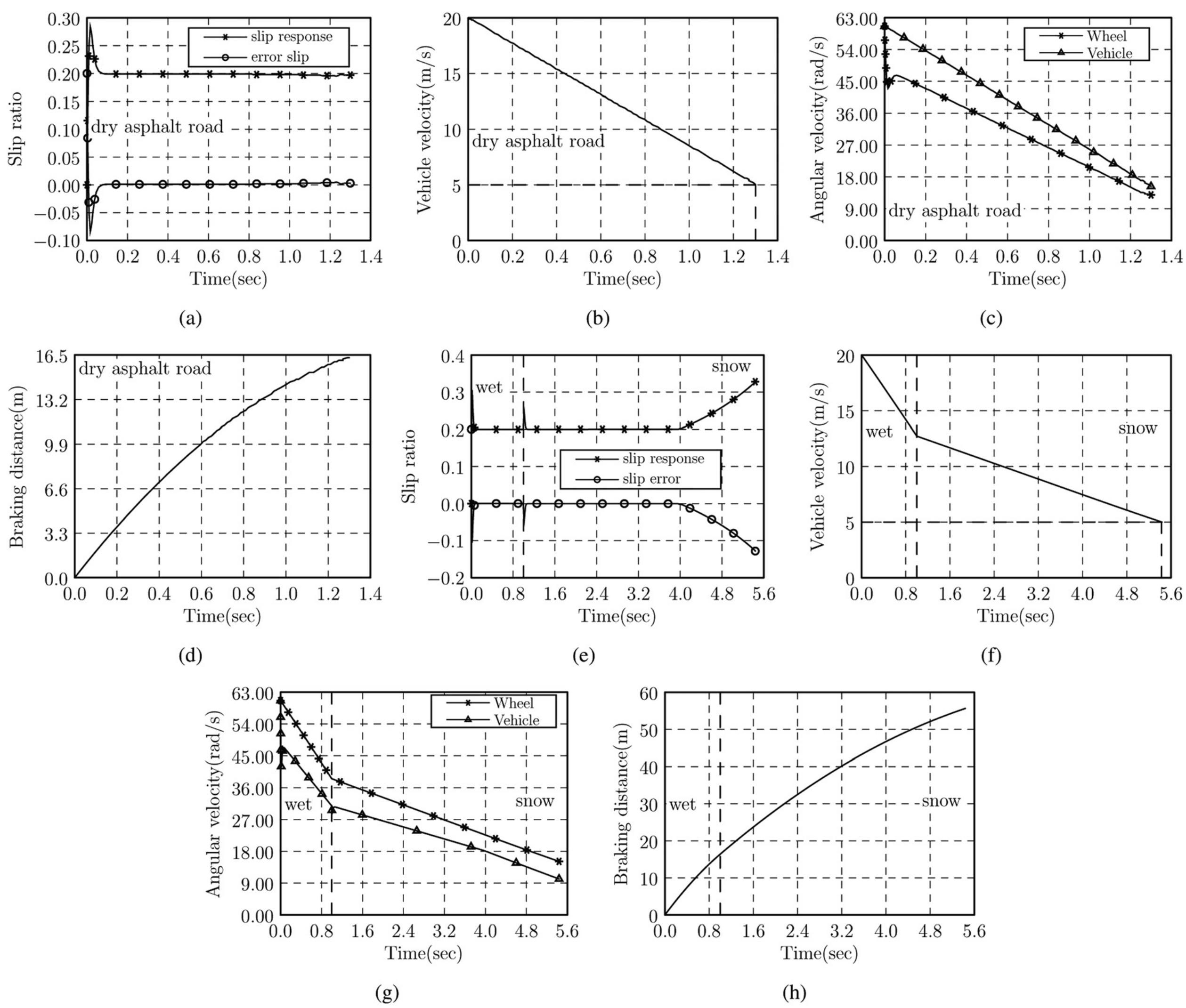

Fig. 5 Simulation results of SMC with PI sliding surface

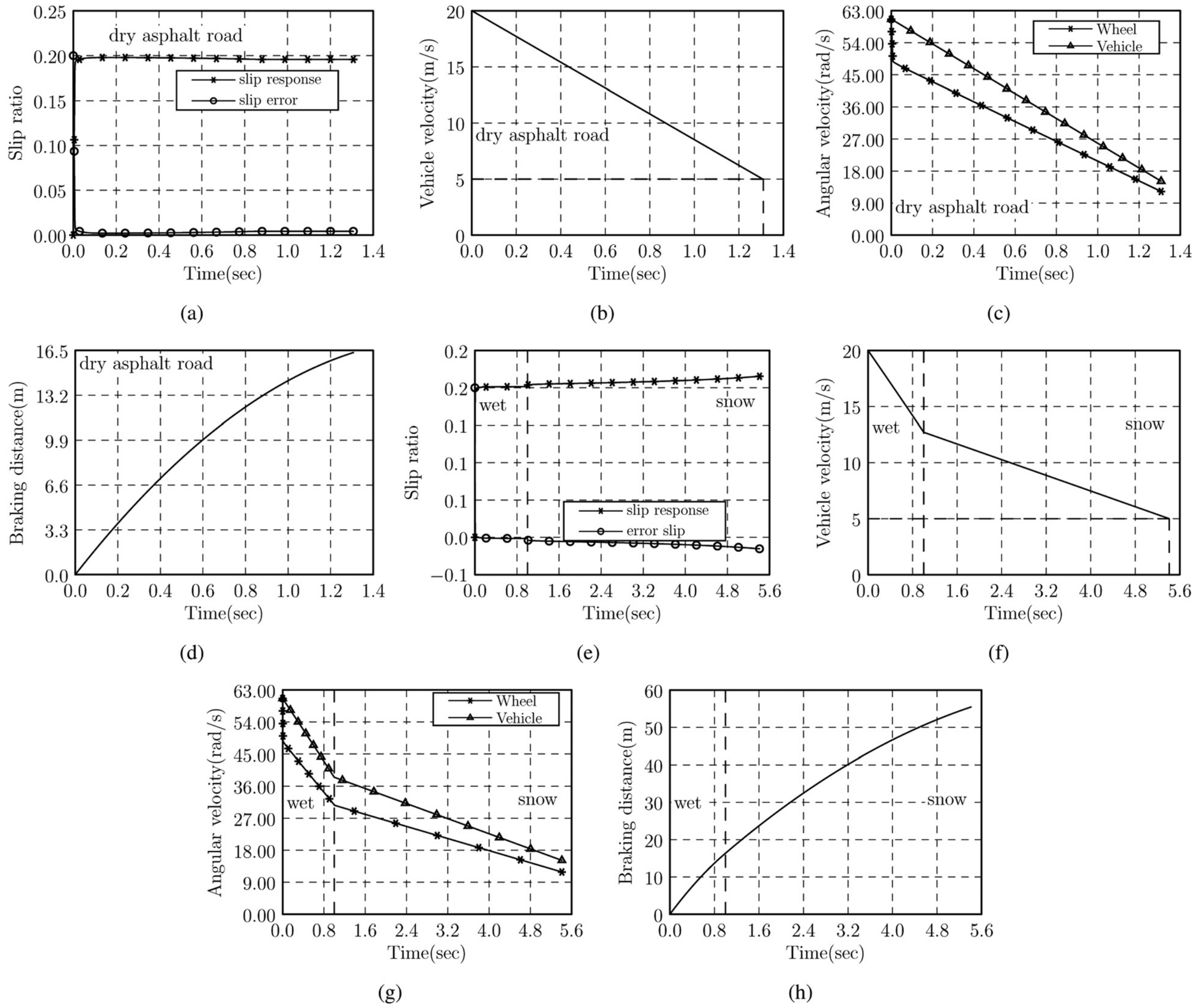

Fig. 6 Simulation results of SMC with PD$^{\alpha}$ sliding surface

First, SMC with PI sliding surface is applied to ABS [32,33]. The simulation results for dry asphalt road and transition from wet asphalt road to snow road are shown in Figs. 5(*a*)–5(*d*) and 5(*e*)–5(*h*) with $\rho = 25$, $k = 100$, $\phi = 0.2$, respectively. From Fig. 5(*a*), it can be seen that the slip response controlled by SMC with PI sliding surface has 42% overshoot, small steady-state error for dry asphalt road. Figure 5(*b*) shows the response curve of vehicle velocity. Figure 5(*c*) shows the angular velocity response curve of vehicle and wheel, respectively. Figure 5(*d*) shows the braking distance when the vehicle velocity reaches 5 m/s. Figure 5(*e*) shows the slip response curve and slip error response curve for road condition transition. It can be seen that it has 50% overshoot when braking on wet asphalt road and 22.5% overshoot when road condition changes from wet asphalt road to snow road at 1s, then the slip ratio goes back to the expected value again, but it fails to perform well after 4 s.

For showing the advantages of fractional-order sliding surface, the SMC with PD$^{\alpha}$ sliding surface presented in Sec. 4 is applied to ABS. The simulation results for dry asphalt road and transition from wet asphalt road to snow road are shown in Figs. 6(*a*)–6(*d*) and 6(*e*)–6(*h*) with $\rho = 80$, $k = 1$, $\alpha = 0.15$, $\phi = 0.0667$, respectively. From Fig. 6(*a*), it can be seen that the slip response has not much overshoot but has some steady-state error. Figure 6(*e*) shows the slip response curve and slip error response curve for road condition transition. It can be seen that there is good performance when braking on wet asphalt road, but the performance when road condition changes from wet asphalt road to snow road at 1 s is not satisfactory. From Figs. 6(*a*)–6(*h*), the performance of SMC with PD$^{\alpha}$ sliding surface is relatively better than that of SMC with PI sliding surface.

Finally, the AFFOSMC presented in Sec. 5 is applied to ABS. The simulation results are shown in Figs. 7(*a*)–7(*d*) for dry asphalt road and Figs. 7(*e*)–7(*h*) for transition from wet asphalt road to snow road with $k = 0.4$, $\alpha = 0.35$, $\eta_1 = 30$, $\eta_2 = 110$, $\phi = 1$. From Fig. 7(*a*), it can be seen that the slip can track the desired value after 0.2 s for the dry asphalt road. From Fig. 7(*b*), it can be seen that the braking time that the vehicle velocity reaches 5 m/s is 1.28 s. And it can be seen from Fig. 7(*d*) that the braking distance is 16.1 m. To sum up, the proposed method can obtain the shortest tracking time, the shortest braking distance, and the shortest braking time for dry asphalt road, and it is superior to the other two methods. From Fig. 7(*e*), it can be seen that the slip response is very well when braking on wet asphalt road and it has only 6.5% overshoot when the road condition changes at 1 s and the slip ratio goes back to the expected value again at around 1.25 s. The braking time that the vehicle velocity reaches 5 m/s is 5.45 s and the braking distance is 56 m for road transition seen from Figs. 7(*f*) and 7(*h*), respectively. It is thus clear that the proposed AFFOSMC performs the best when road transition occurs.

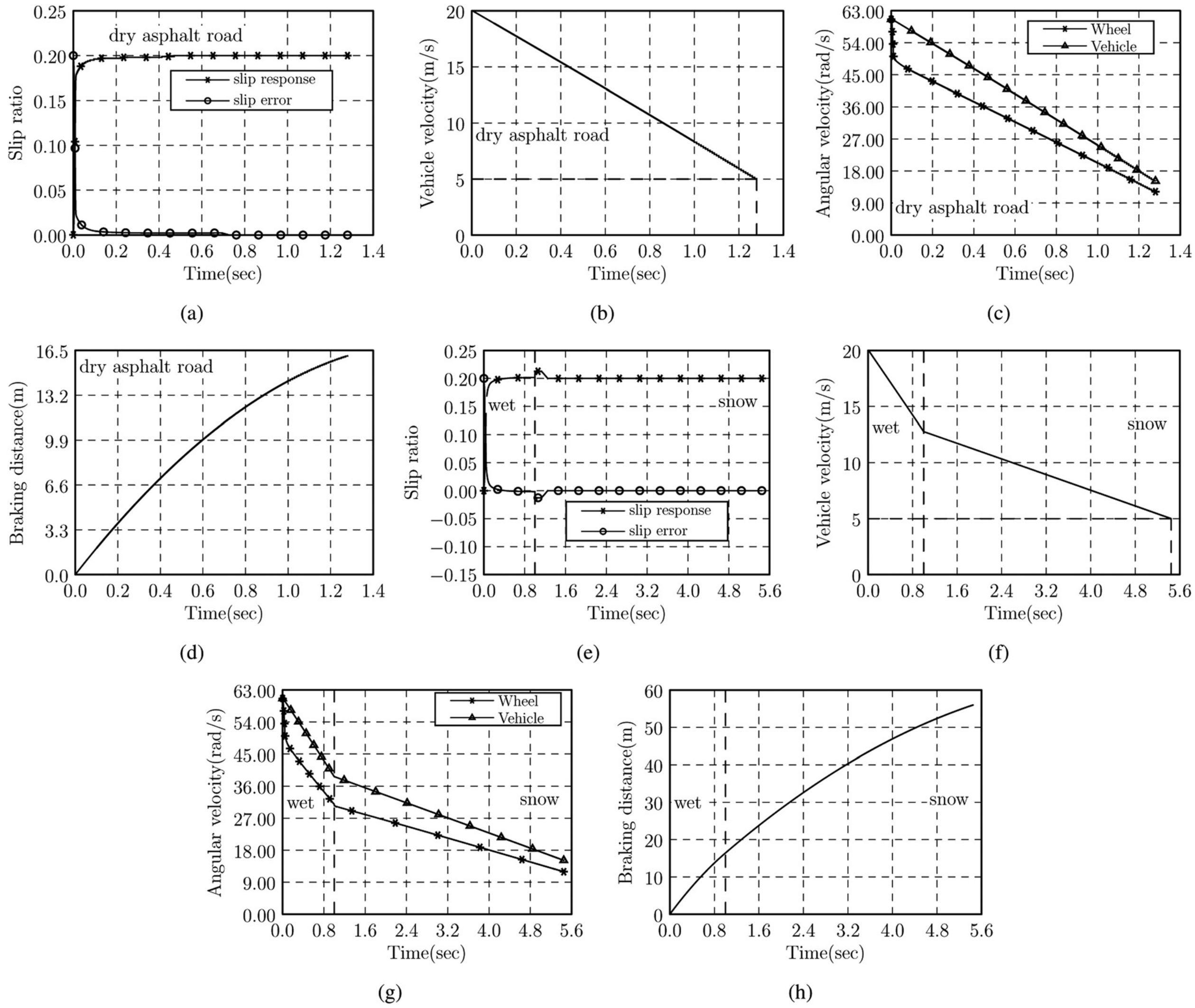

Fig. 7 Simulation results of the proposed method

Table 1 Root-mean-square error (RMSE) of slip response of different controllers

Controller	Dry asphalt road	Wet to snow road
SMC–PI	0.0438	0.0399
SMC–PD$^{\alpha}$	0.0192	0.0191
AFFOSMC	0.0099	0.0098

To compare the performance of the above different controllers quantitatively, the RMSE of slip response is listed in Table 1. It can be seen from Table 1 that RMSE of AFFOSMC is the minimum.

7 Conclusion

In this paper, an AFFOSMC design method is proposed to control ABS. In AFFOSMC, FLC, and FOSMC are integrated to deal with uncertainties and enhance the robustness of the controller. In FOSMC, a fractional-order sliding surface, i.e., PD$^{\alpha}$ sliding surface is adopted. The FC is introduced into FOSMC and consequently, FOSMC has better response speed and is more robust than the traditional SMC. In addition, to deal with the uncertainties arisen from the unknown environmental parameters, an FLC is designed as a compensation controller. The input variables of FLC are the fractional-order sliding surface and its derivative. The adjusting laws of parameters of FLC are derived based on Lyapunov theory, and thus the stability of the whole system can be guaranteed. Simulation results show that the proposed AFFOSMC has faster response speed, less overshoot, and more robust than SMC with PI sliding surface and SMC with PD$^{\alpha}$ sliding surface.

Acknowledgment

This work was supported by the National Natural Science Foundation of China (Nos. 61273260 and 61471313), Natural Science Foundation of Hebei Province (No. F2014203208), the Specialized Research Fund for the Doctoral Program of Higher Education of China (No. 20121333120010), and China Postdoctoral Science Foundation (Nos. 2013M530888 and 2014T70229).

Nomenclature

$B_v =$ the vehicle viscous friction
$B_\omega =$ the viscous friction of the wheel
${}_a\mathrm{D}_t^{\alpha} =$ integrodifferential operator of fractional-order
$E =$ the upper bounds of error between the ideal controller and equivalent controller
$F_t(t) =$ the tractive force
$F_\theta(\theta) =$ the vertical force applied to the car
$h =$ time increment
$J_\omega =$ the rotation inertia of the wheel

$M =$ the mass of the vehicle
$s =$ Laplace operator
$s(t) =$ the sliding surface
$\mathrm{sat}(\cdot) =$ the saturation function
$\mathrm{sgn}(\cdot) =$ the sign function
$T_b(t) =$ the braking torque
$T_t(t) =$ the torque generated due to slip between the wheel and the road surface
$u_{\mathrm{eq}}(t) =$ the equivalent controller in sliding mode control
$u_{\mathrm{rb}}(t) =$ the hitting controller in sliding mode control
$\hat{u}_{fz}(t) =$ the fuzzy controller
$V_v(t) =$ the velocity of the vehicle
$\alpha =$ differentiation order
$\Gamma(\cdot) =$ gamma function
$\eta_1 =$ the learning rate of parameters of fuzzy controller
$\eta_2 =$ the learning rate of error's upper bounds E
$\theta =$ the angle of inclination
$\lambda(t) =$ the slip of wheel
$\lambda_d(t) =$ the desired slip
$\lambda_e(t) =$ the error of slip between the desired slip and the actual slip of wheel
$\mu =$ the friction coefficient of road
$\phi =$ the width of boundary layer
$\omega_b =$ lower limits of frequency of Oustaloup approximation
$\omega_h =$ upper limits of frequency of Oustaloup approximation
$\omega_v(t) =$ the angle velocity of the vehicle
$\omega_\omega(t) =$ the angular velocity of the wheel

References

[1] Oudghiri, M., Chadli, M., and Hajjaji, A. E., 2007, "Robust Fuzzy Sliding Mode Control for Antilock Braking System," Int. J. Sci. Tech. Autom. Control, **1**, pp. 13–28.
[2] Hoseinnezhad, R., and Hadiashar, A. B., 2011, "Efficient Antilock Braking by Direct Maximization of Tire-Road Frictions," IEEE Trans. Ind. Electron., **58**(8), pp. 3593–3599.
[3] Drakunov, S., Ümit Özgüner, Dix, P., and Ashrafi, B., 1995, "ABS Control Using Optimum Search Via Sliding Modes," IEEE Trans. Control Syst. Technol., **3**(1), pp. 79–85.
[4] Liu, Y., and Sun, J., 1995, "Target Slip Tracking Using Gain-Scheduling for Braking Systems," American Control Conference, Seattle, WA, June 21–23, pp. 1178–1182.
[5] Tan, H.-S., and Tomizuka, M., 1990, "Discrete-Time Controller Design for Robust Vehicle Traction," IEEE Control Syst. Mag., **10**(3), pp. 107–113.
[6] Jing, H., Liu, Z., and Chen, H., 2011, "A Switched Control Strategy for Antilock Braking System With On/Off Valves," IEEE Trans. Veh. Technol., **60**(4), pp. 1470–1484.
[7] Lee, K., and Park, K., 1999, "Optimal Robust Control of a Contactless Brake System Using an Eddy Current," Mechatronics, **9**(6), pp. 615–631.
[8] Oustaloup, A., 1991, *La commande CRONE: Commande robuste d'order non entier*, Hermès, Paris.
[9] Podlubny, I., 1999, *Fractional Differential Equations*, Academic Press, San Diego, CA.
[10] Oldham, K. B., and Spanier, J., 1974, *The Fractional Calculus*, Academia, New York.
[11] Lurie, B. J., 1994, *Three-Parameter Tunable Tilt-Integral-Derivative (TID) Controller*, U.S. Patent No. 5371670.
[12] Oustaloup, A., Lanusse, P., and Mathieu, B., 1995, "Robust Control of SISO Plants: The CRONE Control," Proceedings of the ECC'95 Conference, Kluwer Academic Publishers, Dordrecht, The Netherlands, p. 1423.
[13] Podlubny, I., 1999, "Fractional-Order Systems and $PI^{\lambda}D^{\mu}$ Controllers," IEEE Trans. Autom. Control, **44**(1), pp. 208–214.
[14] Efe, M. O., 2011, "Integral Sliding Mode Control of a Quadrotor With Fractional-Order Reaching Dynamics," Trans. Inst. Meas. Control, **33**(8), pp. 985–1003.
[15] Efe, M. O., 2008, "Fractional Fuzzy Adaptive Sliding-Mode Control of a 2-DOF Direct Drive Robot Arm," IEEE Trans. Syst. Man Cybern. Part B Cybern., **38**(6), pp. 1561–1570.
[16] Delavari, H., Ghadri, R., Ranjbar, A., and Momani, S., 2010, "Fuzzy Fractional-Order Sliding Mode Controller for Nonlinear Systems," Commun. Nonlinear Sci. Numer. Simul., **15**(4), pp. 963–978.
[17] Lee, C., 1990, "Fuzzy Logic in Control Systems: Fuzzy Logic Controller. II," IEEE Trans. Syst. Man Cybern., **20**(2), pp. 404–418.
[18] Huang, C. H., Wang, W. J., and Chiu, C. H., 2011, "Design and Implementation of Fuzzy Control on a Two-Wheel Inverted Pendulum," IEEE Trans. Ind. Electron., **58**(7), pp. 2988–3001.
[19] Lin, C. M., and Li, H. Y., 2012, "A Novel Adaptive Wavelet Fuzzy Cerebellar Model Articulation Control System Design for Voice Coil Motors," IEEE Trans. Ind. Electron., **59**(4), pp. 2024–2033.
[20] Precup, R., David, R., Petriu, E., Preitl, S., and Radac, M., 2012, "Fuzzy Control Systems With Reduced Parametric Sensitivity Based on Simulated Annealing," IEEE Trans. Ind. Electron., **59**(8), pp. 3049–3061.
[21] Layne, J., Passino, K., and Yurkovich, S., 1993, "Fuzzy Learning Control for Antiskid Braking Systems," IEEE Trans. Control Syst. Technol., **1**(2), pp. 122–129.
[22] Mauer, G. F., 1995, "A Fuzzy Logic Controller for an ABS Braking System," IEEE Trans. Fuzzy Syst., **3**(4), pp. 381–388.
[23] Kim, S. W., and Lee, J. J., 1995, "Design of a Fuzzy Controller With Fuzzy Sliding Surface," Fuzzy Sets Syst., **71**(3), pp. 359–367.
[24] Kayacan, E., Cigdem, O., and Kaynak, O., 2012, "Sliding Mode Control Approach for Online Learning as Applied to Type-2 Fuzzy Neural Networks and Its Experimental Evaluation," IEEE Trans. Ind. Electron., **59**(9), pp. 3510–3520.
[25] Tang, Y., Zhang, X., Zhang, D., Zhao, G., and Guan, X., 2013, "Fractional-Order Sliding Mode Controller Design for Antilock Braking Systems," Neurocomputing, **111**, pp. 122–130.
[26] Podlubny, I., 1999, "Fractional-Order Systems and $PI^{\lambda}D^{\mu}$ Controllers," IEEE Trans. Autom. Control, **44**(1), pp. 208–214.
[27] Diethelm, K., Ford, N., and Freed, A. D., 2002, "A Predictor–Corrector Approach for the Numerical Solution of Fractional Differential Equations," Nonlinear Dyn., **29**, pp. 3–22.
[28] Shampine, L. F., and Gordon, M. K., 1975, *Computer Solution of Ordinary Differential Equations: The Initial Value Problem*, W. H. Freeman & Co., San Francisco, CA.
[29] Matignon, D., 1998, "Stability Properties for Generalized Fractional Differential Systems," ESAIM: Proc., **5**, pp. 145–158.
[30] Poursamad, A., 2009, "Adaptive Feedback Linearization Control of Antilock Braking Systems Using Neural Networks," Mechatronics, **19**(5), pp. 767–773.
[31] Lin, C. M., and Hsu, C. F., 2003, "Neural Network Hybrid Control for Antilock Braking Systems," IEEE Trans. Neural Networks, **14**(2), pp. 351–359.
[32] Lin, C.-M., and Hsu, C. F., 2003, "Self-Leaning Fuzzy Sliding Mode Control for Anti-Lock Braking Systems," IEEE Trans. Control Syst. Technol., **11**(2), pp. 273–278.
[33] Harifi, A., Aghagolzadeh, A., Alizadeh, G., and Sadeghi, M., 2005, "Designing a Sliding Mode Controller for Antilock Brake System," IEEE The International Conference on Computer as a Tool, EUROCON 2005, Belgrade, Serbia, Nov. 21–24, Vol. 1, pp. 258–261.